

Influence of the substituent R^1 on the reactivity of $[(\eta^5\text{-C}_5\text{H}_5)\text{Fe}\{(\eta^5\text{-C}_5\text{H}_4)\text{-CH=N-(R}^1\text{)-OH}\}]$ $\{R^1 = \text{-CH}_2\text{-CH}_2\text{- or 1,2-C}_6\text{H}_4\}$ with platinum(II) and on the properties of the complexes†

Concepción López,^{*a} Sonia Pérez,^a Xavier Solans,^b Mercè Font-Bardía^b and Teresa Calvet^b

Received (in Victoria, Australia) 14th July 2009, Accepted 5th November 2009

First published as an Advance Article on the web 28th January 2010

DOI: 10.1039/b9nj00509a

The synthesis and characterization of four different types of platinum(II) complexes derived from $[(\eta^5\text{-C}_5\text{H}_5)\text{Fe}\{(\eta^5\text{-C}_5\text{H}_4)\text{-CH=N-(CH}_2\text{-CH}_2\text{-OH)}\}]$ (**1b**) are reported. The new products are the *trans*- and *cis*-isomers of $[\text{Pt}\{(\eta^5\text{-C}_5\text{H}_5)\text{Fe}\{(\eta^5\text{-C}_5\text{H}_4)\text{-CH=N-(CH}_2\text{-CH}_2\text{-OH)}\}\text{Cl}_2(\text{dmsO})]$ $\{trans\text{-}(\mathbf{2b})$ and *cis*- $(\mathbf{3b})\}$ and the platinacycles $[\text{Pt}\{[(\eta^5\text{-C}_5\text{H}_5)\text{-CH=N-(CH}_2\text{-CH}_2\text{-OH)}]\text{Fe}(\eta^5\text{-C}_5\text{H}_5)\text{Cl}(\text{L})]$ $\{with L = \text{dmsO} (\mathbf{4b})$ or $\text{PPh}_3 (\mathbf{5b})\}$ or $[\text{Pt}\{[(\eta^5\text{-C}_5\text{H}_5)\text{-CH=N-(CH}_2\text{-CH}_2\text{-O)}]\text{Fe}(\eta^5\text{-C}_5\text{H}_5)\text{Cl}(\text{L})]$ $\{with L = \text{PPh}_3 (\mathbf{6b})$ or $\text{dmsO} (\mathbf{7b})\}$. In these products **1b** acts as a (N) donor ligand (in **2b** and **3b**), as a bidentate $[\text{C}(\text{sp}^2, \text{ferrocene}), \text{N}]^-$ (in **4b** and **5b**) or as a terdentate $[\text{C}(\text{sp}^2, \text{ferrocene}), \text{N}, \text{O}]^{2-}$ ligand (in **6b** and **7b**). The crystal structures of **4b** and **5b** confirm the mode of binding of the ferrocenylaldimine (**1b**) and a *trans*-arrangement between the neutral ligand (L) and the imine nitrogen. Comparative studies of: (a) the reactivity of ligands $[(\eta^5\text{-C}_5\text{H}_5)\text{Fe}\{(\eta^5\text{-C}_5\text{H}_4)\text{-CH=N-(R}^1\text{)-OH}\}]$ $\{R^1 = \text{-CH}_2\text{-CH}_2\text{- or 1,2-C}_6\text{H}_4\}$ with *cis*- $[\text{PtCl}_2(\text{dmsO})_2]$ and (b) the properties of their platinum(II) complexes are also reported and provide conclusive evidence of the influence of the nature of the R^1 group of $[(\eta^5\text{-C}_5\text{H}_5)\text{Fe}\{(\eta^5\text{-C}_5\text{H}_4)\text{-CH=N-(R}^1\text{)-OH}\}]$ on: (a) the spectroscopic and electrochemical properties of these ligands and their platinum(II) complexes, (b) the cycloplatination process, and (c) the ease with which the mode of binding of the ligand changes from bidentate $[\text{C}(\text{sp}^2, \text{ferrocene}), \text{N}]^-$ to terdentate $[\text{C}(\text{sp}^2, \text{ferrocene}), \text{N}, \text{O}]^{2-}$ or *vice versa*.

Introduction

Organometallic platinum(II) compounds containing bidentate $\{[\text{C}, \text{E}]^-\}$ (E = N, S, P)^{1,2} or terdentate $\{[\text{X}, \text{C}, \text{X}']^-\}$ (X = N, S, or P) or $[\text{C}, \text{N}, \text{X}'^q]$ (X' = N', $q = -1$ or X' = S or O and $q = -1$ or -2)^{1,3} ligands have attracted great interest recently due to their physical, photo-optical and chemical properties, their antitumoral and catalytic activity and their utility in macro- and supramolecular chemistry, organic and organometallic synthesis and homogeneous catalysis.^{1–3}

On the other hand, despite the interest of platinum(II) complexes with ferrocene derivatives as ligands and the prochiral nature of the ferrocenyl moiety in the cyclometalation process,⁴ compounds with “ $\text{Pt}[\text{C}(\text{sp}^2, \text{ferrocene}), \text{N}, \text{O}]^q$ ($q = -1$ or -2)” cores are scarce.⁵ Among the examples known, those derived from $[(\eta^5\text{-C}_5\text{H}_5)\text{Fe}\{(\eta^5\text{-C}_5\text{H}_4)\text{-CH=N-(C}_6\text{H}_4\text{-2-OH)}\}]$ (**1a**) (Fig. 1) are especially relevant due to their behaviour as pH-based molecular switches.^{5b} In view of this and in order to determine the effect induced by the nature of the unit R^1 of $[(\eta^5\text{-C}_5\text{H}_5)\text{Fe}\{(\eta^5\text{-C}_5\text{H}_4)\text{-CH=N-(R}^1\text{)-OH}\}]$ $\{R^1 = 1,2\text{-C}_6\text{H}_4$

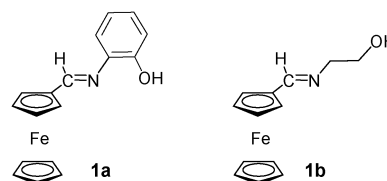


Fig. 1 Chemical formulae of the ferrocenyl Schiff bases: $[(\eta^5\text{-C}_5\text{H}_5)\text{Fe}\{(\eta^5\text{-C}_5\text{H}_4)\text{-CH=N-(R}^1\text{)-OH}\}]$ with $R^1 = 1,2\text{-C}_6\text{H}_4$ (**1a**) or $\text{-CH}_2\text{-CH}_2\text{-}$ (**1b**).

(**1a**) or $\text{-CH}_2\text{-CH}_2\text{-}$ (**1b**), Fig. 1) on: (a) their reactivity in front of platinum(II), (b) the properties of the platinacycles containing **1a** or **1b** acting as $[\text{C}(\text{sp}^2, \text{ferrocene}), \text{N}, \text{O}]^{2-}$ and $[\text{C}(\text{sp}^2, \text{ferrocene}), \text{N}]^-$ ligands and (c) the utility of the platinacycles as pH-dependent molecular switches. Here we present the study of the reactivity of $[(\eta^5\text{-C}_5\text{H}_5)\text{Fe}\{(\eta^5\text{-C}_5\text{H}_4)\text{-CH=N-(CH}_2\text{-CH}_2\text{-OH)}\}]$ (**1b**)⁶ (Fig. 1) with *cis*- $[\text{PtCl}_2(\text{dmsO})_2]$ ⁷ as well as a comparative study of the effect of the R^1 group on the properties of the platinacycles derived from **1b** and **1a**.

Results and discussion

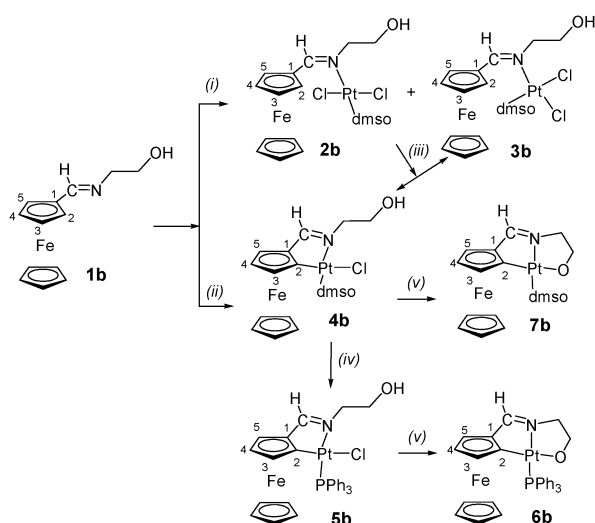
Synthesis

In order to facilitate the reading, a summary of the reactions studied is presented in Scheme 1 and Table 1. For comparison purposes the conditions used previously to isolate

^a Departament de Química Inorgànica, Facultat de Química, Universitat de Barcelona, Martí i Franquès 1-11, 08028-Barcelona, Spain. E-mail: conchi.lopez@qi.ub.es; Fax: +34 934907725; Tel: +34 934039134

^b Departament de Cristal·lografia, Mineralogia i Dipòsits Minerals, Facultat de Geologia, Universitat de Barcelona, Martí i Franquès s/n, 08028-Barcelona, Spain

† CCDC reference numbers 734801 and 734802. For crystallographic data in CIF or other electronic format see DOI: 10.1039/b9nj00509a



Scheme 1 (i) *Cis*-[PtCl₂(dmsO)₂] {molar ratio **1b**:Pt(II) = 1} in refluxing MeOH. The molar ratio **2b**:**3b** is dependent on the refluxing period (see text). (ii) *Cis*-[PtCl₂(dmsO)₂] and NaAcO {molar ratios **1b**:Pt(II):AcO⁻ = 1:1:2} in a mixture toluene:MeOH (5:1) under reflux followed by a SiO₂ column chromatography (see text). (iii) Treatment with an equimolar amount of NaAcO in refluxing MeOH for 120 h. (iv) Addition of PPh₃ {in a molar ratio **4b**:PPh₃ = 1} in benzene at 343 K for 1.5 h, followed by a SiO₂ column chromatography. (v) In CDCl₃ (or CH₂Cl₂) followed by the addition of NaOD (or MeOH) (see text).

trans-[Pt{(η⁵-C₅H₅)Fe{(η⁵-C₅H₄)-CH=N-(CH₂-CH₂-OH)}]Cl₂(dmsO)] (**2b**)⁶ are also included in Table 1, entry I.

In a first attempt to achieve cycloplatinated complexes, ligand **1b**⁶ was treated with an equimolar amount of *cis*-[PtCl₂(dmsO)₂]⁷ in refluxing methanol for 20 h [Table 1, entry II and Scheme 1, step (i)]. After the work up of a SiO₂ column chromatography three products were isolated. The minor components were identified as ferrocenecarboxaldehyde† (hereinafter referred to as FcCHO) and **2b**; while characterization data of the major product (**3b**) agreed with those expected for the *cis*-isomer of [Pt{(η⁵-C₅H₅)Fe{(η⁵-C₅H₄)-CH=N-(CH₂-CH₂-OH)}]Cl₂(dmsO)]. However, no evidence of the formation of any platinumacycle was detected by ¹H-NMR.

In view of this, and since it has been reported that the formation of metallacycles with [C(sp², ferrocene), N]⁻ or [C(sp², ferrocene), N, X]⁻ (X = N', S) ligands is often favoured in the presence of an excess of base,^{5,8-10} we also studied the reaction of **1b**, *cis*-[PtCl₂(dmsO)₂] and NaAcO (in a molar ratio of 1:1:2) in a toluene-methanol (5:1) mixture under reflux for 72 h. After the work-up, four compounds were obtained, two of them were **2b** and **3b**, and one of the minor components was FcCHO (Table 1, entry III). Characterization data of the fourth product (**4b**) agreed with those expected for the platinumacycle [Pt{(η⁵-C₅H₅)-CH=N-(CH₂-CH₂-OH)]Fe(η⁵-C₅H₅)]Cl(dmsO)]. The crystal structure of **4b**

† FcCHO arises from the hydrolysis of the imine. The formation of FcCHO or C₆H₅CHO as side-products has also been detected in cycloplatinated complexes of other ferrocenylaldimines^{5,6,8} or the diimine (1*R*,2*R*)-1,2-[(C₆H₅-CH=N)]₂-C₆H₁₀] (J. Bravo, C. Cativela, R. Navarro and E. P. Urriolabeitia, *J. Organomet. Chem.* 2002, **650**, 157-172).

(*vide infra*) confirmed that the aldimine (**1b**) behaved as a [C(sp², ferrocene), N]⁻ ligand. These results are in sharp contrast with those obtained for [(η⁵-C₅H₅)Fe{(η⁵-C₅H₄)-CH=N-(C₆H₄-2-OH)}] (**1a**), that under identical experimental conditions, gave [Pt{(η⁵-C₅H₅)-CH=N-(C₆H₄-2-O)-Fe(η⁵-C₅H₅)](dmsO)] with a *mer*-terdentate [C(sp², ferrocene), N, O]²⁻ ligand.^{5b}

The yield of **4b** improved substantially when the reaction period (*t*) increased from 72 h to 120 h {Table 1, entries III and IV, respectively and Scheme 1, step (ii)} and the relative abundance of **2b** and **3b** decreased. Thus, the separation of **4b** was easier.

Furthermore, the reaction of **2b** with the equimolar amount of NaAcO in refluxing methanol for 120 h also produced a mixture of **3b** and **4b** {Scheme 1, step (iii)}, but the molar ratio **4b**:**3b** (3.2:1.0) was smaller than that obtained when **1b** was treated with *cis*-[PtCl₂(dmsO)₂] and a two-fold excess of NaAcO (Table 1, entry IV, molar ratio **4b**:**3b** = 7.1:1.0).

Further treatment of **4b** with an equimolar amount of PPh₃ in benzene at 343 K, gave [Pt{(η⁵-C₅H₅)-CH=N-(CH₂-CH₂-OH)]Fe(η⁵-C₅H₅)]Cl(PPh₃) (**5b**) {Scheme 1, step (iv)}. Despite the poor quality of the crystals obtained the structural studies (see below) confirmed: (a) a *cis*-arrangement between the phosphine and the metallated carbon and (b) the mode of binding of the ligand, [C(sp², ferrocene), N]⁻, in **5b**.

It should be noted that no evidence of the opening of the metallacycle was detected by NMR even when the molar ratio PPh₃:**5b** was 2.0:1.0. This suggested that the Pt-N bond of **4b** and **5b** exhibits low lability.

Due to the increasing interest in platinumacycles with pincer ligands^{1,3,5,8a,10} and since **4b** and **5b** contain an alcohol unit on the pendant arm we decided to determine whether the presence of a base could induce the formation of platinum(II) complexes with "Pt{C(sp², ferrocene), N, O}" cores.

In a first attempt, we studied the action of NaOD (in MeOD) on a CDCl₃ solution of **5b** and monitored the changes by ³¹P{¹H}-NMR (Fig. 2, A-D). The addition of NaOD (in MeOD) to a freshly prepared solution of **5b** in CDCl₃ at 298 K in molar ratios NaOD:**5b** varying from 0.2:1.0 to 0.7:1.0} did not produce significant changes in the ³¹P{¹H}-NMR spectra. However, when larger excesses of NaOD were added (molar ratios from 0.9:1.0 to 1.5:1.0), the signals detected in the spectra (Fig. 2, B and C) indicated the presence of two different species in solution one of them being unreacted **5b**. The chemical shift of the new singlet (δ = 16.3 ppm) as well as the value of the coupling constant (¹J_{P-Pt} = 3498 Hz) suggested, according to the literature,^{5b} the presence of [Pt{(η⁵-C₅H₅)-CH=N-(CH₂-CH₂-O)]Fe(η⁵-C₅H₅)](PPh₃) (**6b**), with a [C(sp², ferrocene), N, O]²⁻ ligand. The complete transformation of **5b** into **6b** was achieved when the molar ratio NaOD:**5b** was 1.8:1.0 {Fig. 2, D and Scheme 1, step (v)}.

Similarly, when a CDCl₃ solution of **4b** was treated at 298 K with NaOD (in MeOD and in a molar ratio NaOD:**4b** = 1.8:1.0), the ¹H-NMR spectrum of the resulting solution (Fig. 3), suggested the formation of [Pt{(η⁵-C₅H₅)-CH=N-(CH₂-CH₂-O)]Fe(η⁵-C₅H₅)](dmsO)] (**7b**) (Scheme 1). However, when the same experiment was carried out using **3b** instead of **4b** or **5b** the ¹H-NMR spectrum of the resulting solution revealed the presence of large amounts of FcCHO.

Table 1 Summary of the experimental conditions [reagents, solvents, temperature (T) and reaction time (t , in h)] used in the study of the reactivity of $[(\eta^5\text{-C}_5\text{H}_5)\text{Fe}\{(\eta^5\text{-C}_5\text{H}_4)\text{-CH=N-(CH}_2\text{-CH}_2\text{-OH)}\}]$ (**1b**) with *cis*-[PtCl₂(dmsO)₂] (abbreviated as [Pt])

Entry	Reagents (molar ratio)	Solvent	T	t	Products ^a (molar ratio)
I	1b and [Pt] (1 : 1)	MeOH	Reflux	3	2b ^b
II	1b and [Pt] (1 : 1)	MeOH	Reflux	20	2b and 3b (0.36 : 1.00)
III	1b , [Pt] and NaAcO (1 : 1 : 2)	Toluene/MeOH ^c	Reflux	72	2b , 3b and 4b (0.24 : 1.0) ^d
IV	1b , [Pt] and NaAcO (1 : 1 : 2)	Toluene/MeOH ^c	Reflux	120	2b , 3b and 4b (0.05 : 0.14 : 1.00)

^a In these reactions small amounts of FeCHO were also isolated as by-product. ^b Data from ref. 6. ^c A (5 : 1) mixture. ^d In this case traces (12 mg) of **4b** were obtained.

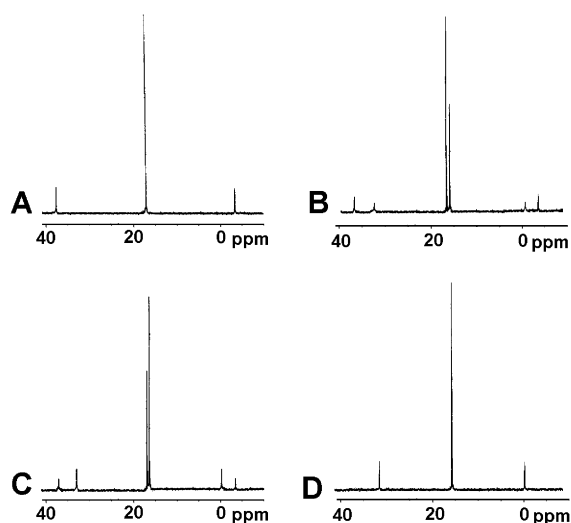


Fig. 2 ³¹P{¹H}-NMR spectrum (in the range $-10 \text{ ppm} < \delta < 40 \text{ ppm}$) of a freshly prepared solution of [Pt{[($\eta^5\text{-C}_5\text{H}_3$)-CH=N-(CH₂-CH₂-OH)]Fe($\eta^5\text{-C}_5\text{H}_5$)}Cl(PPh₃)] (**5b**) in CDCl₃ (A) and after the addition of NaOD (in MeOD) in molar ratios NaOD : **5b** = 1.0 : 1.0 (B), 1.5 : 1.0 (C) and 1.8 : 1.0 (D).

It should be noted that the transformations **5b** → **6b** (or **4b** → **7b**) are slower than **5a** → **6a** (or **4a** → **7a**) and require a larger excess of NaOD {molar ratios NaOD : (**5b** or **4b**) = 1.8 : 1.0 versus NaOD : (**5a** or **4a**) = 1.0 : 1.0^{5b}}.

In order to complete the characterization of **6b** and **7b**, products **5b** and **4b**, were treated separately in CH₂Cl₂ with NaOH {molar ratio NaOH : (**4b** or **5b**) = 1.8 : 1.0} dissolved in methanol at 298 K {Scheme 1, steps (v)}. After work up a deep-purple (for **6b**) or a garnet (for **7b**) solid was isolated. Elemental analyses of **6b** and **7b** agreed with the proposed formulae. Their IR spectra showed the typical band of the >C=N- group¹¹ [at 1569 (for **6b**) and 1575 cm⁻¹ (for **7b**)], but that due to the stretching of the -OH unit was not detected. This suggested: (a) the deprotonation of the alcohol group and (b) the existence of the Pt-O bond in **6b** and **7b**.

In the ¹H-NMR spectra of freshly prepared solutions of **6b** and **7b** in CDCl₃ the signals were slightly broader than expected, in particular when compared with those of **5b** and **4b**, respectively. Besides, when the ³¹P{¹H}-NMR spectrum of a CDCl₃ solution of **6b** was registered after 1 h in solution at 298 K the signals due to **5b** ($\delta = 17.1 \text{ ppm}$, $^1J_{\text{P-Pt}} = 4017 \text{ Hz}$) were also detected. These findings suggested that in **6b** and **7b** the Pt-O bond is labile.

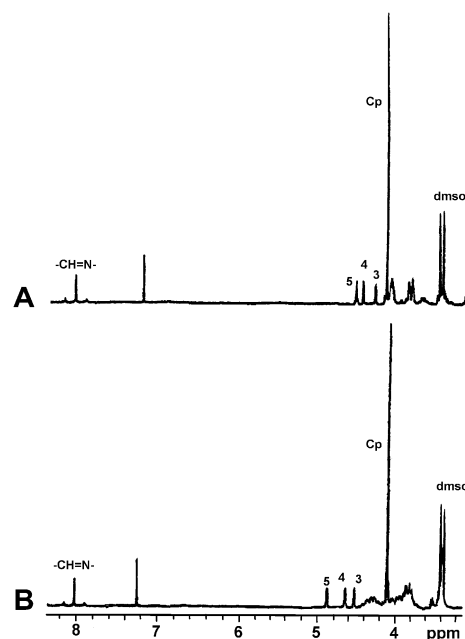


Fig. 3 ¹H-NMR spectra (400 MHz) of a freshly prepared solution of **4b** in CDCl₃ (A) and after the addition of NaOD (in MeOD) in a molar ratio NaOD : **4b** = 1.8 : 1.0 (B) (Cp represents the C₅H₅ ring).

Characterization of the compounds

The new products (**3b**–**7b**) were characterized by elemental analyses, mass spectrometry, infrared and UV-vis spectroscopies and NMR spectroscopy. In all cases elemental analyses (see Experimental) were consistent with the proposed formulae.

The most relevant features observed in the IR spectra are: (a) the existence of the typical band due to the stretching of the imine group^{5,6,8,10,11} and (b) the presence of the absorptions of the S-bonded dmsO ligand (in **3b**, **4b** and **7b**),¹² or the X-sensitive bands of PPh₃ (in **5b** and **6b**)¹³ in platinumacyles [Pt(C,N)Cl(PPh₃) or [Pt(C,N,O)(PPh₃)].⁵ An intense band in the range 3460–3490 cm⁻¹, assigned to the stretching of the $\sigma(\text{O-H})$ bond, was also observed in the IR spectra of compounds **3b**–**5b**. According to the literature,¹⁴ the position of this absorption suggested the existence of intermolecular hydrogen interactions in the solid state.¹⁴ The crystal structures of **4b** and **5b** (see below) confirmed this finding. It should be noted that the absence of the band due to the stretching of the O-H bond in the IR spectrum of **6b** and **7b** agreed with the existence of the Pt-O_{alcoxo} bond.

The assignment of the signals observed in the ^1H and $^{13}\text{C}\{^1\text{H}\}$ -NMR spectra (see Experimental) was achieved with the aid of two-dimensional NMR experiments [$\{^1\text{H}-^1\text{H}\}$ NOESY and COSY and $\{^1\text{H}-^{13}\text{C}\}$ HSQC and HMBC]. Proton and $^{13}\text{C}\{^1\text{H}\}$ -NMR spectra showed the typical pattern of mono-(for **3b**) or 1,2-disubstituted ferrocene derivatives (for **4b-7b**).^{4-6,8-11}

In the ^1H -NMR spectra the resonance of the imine proton appeared as a singlet (for **3b**, **4b** and **7b**) or as a doublet (for **5b** and **6b**) and exhibited the typical satellites due to ^{195}Pt coupling. This is consistent with the presence of the $\sigma(\text{Pt}-\text{N}_{\text{imine}})$ bond. The spectra of **3b**, **4b** and **7b** showed two singlets in the range 2.90–3.60 ppm that are attributed to the dmsoligand. As expected,^{5,8,10} the resonance due to the metallated carbon (C^2) of **4b** and **5b** appeared at lower fields than for the free ligand or compounds **2b** and **3b**.

The chemical shifts of the signals observed in the $^{31}\text{P}\{^1\text{H}\}$ -NMR spectra of **5b** $\{\delta = 17.1, ^1J_{\text{P-Pt}} = 4017 \text{ Hz}\}$ and **6b** $\{\delta = 16.3 \text{ ppm}, ^1J_{\text{P-Pt}} = 3498 \text{ Hz}\}$ are consistent with a *cis*-arrangement between the metallated carbon and the phosphorous of the PPh_3 ligand in good agreement with the so-called transphobia effect.¹⁵ The differences detected in the position of these signals $\{\Delta\delta = (\delta_{\text{for } 5b} - \delta_{\text{for } 6b}) \approx 0.8 \text{ ppm}\}$ is similar to those reported for **5a** ($\delta = 16.2 \text{ ppm}$) and **6a** ($\delta = 15.5 \text{ ppm}$).^{5b}

$^{195}\text{Pt}\{^1\text{H}\}$ -NMR spectra of **2b-5b**[§] provided convincing evidence of: (a) the relative arrangement of the monodentate ligands in **2b** and **3b** and (b) the mode of binding of the ligand $\{(\text{N})\text{-donor (in } 3b) \text{ or } [\text{C}(\text{sp}^2, \text{ferrocene}), \text{N}]^- \text{ (in } 4b \text{ and } 5b)\}$. The variation observed in the chemical shift of **2b** and **3b** ($\Delta\delta = \delta_{\text{for } 3b} - \delta_{\text{for } 2b}$) falls in the range expected for other pairs of *cis*- and *trans*-isomers of complexes of general formulae: $[\text{PtCl}_2(\text{N-donor ligand})_2]$ or $[\text{PtCl}_2(\text{N-donor ligand})(\text{L}')]$ ($\text{L}' = \text{monodentate ligand}$).¹⁶⁻¹⁸

The differences detected in the $^{195}\text{Pt}\{^1\text{H}\}$ -NMR spectra of the pairs of compounds $[\text{Pt}\{[(\eta^5\text{-C}_5\text{H}_3)\text{-CH=N-(R}^1\text{)-OH}]\}\text{Fe}(\eta^5\text{-C}_5\text{H}_5)\text{Cl}(\text{L})]$ with $\text{L} = \text{dmsol}$ [$\text{R}^1 = \text{-CH}_2\text{-CH}_2\text{-}$ (**4b**) ($\delta = -3791 \text{ ppm}$) or 1,2- C_6H_4 (**4a**) ($\delta = -3831 \text{ ppm}$)^{5b}] or $\text{L} = \text{PPh}_3$ [$\text{R}^1 = \text{-CH}_2\text{-CH}_2\text{-}$ (**5b**) ($\delta = -4180 \text{ ppm}, ^1J_{\text{Pt-P}} = 4017 \text{ Hz}$) or 1,2- C_6H_4 (**5a**) ($\delta = -4206 \text{ ppm}, ^1J_{\text{Pt-P}} = 4233 \text{ Hz}$)^{5b}] can be ascribed to the nature of the R^1 group. Since it is well-known that an upfield shift of the signal detected in the $^{195}\text{Pt}\{^1\text{H}\}$ -NMR spectra is related to a strong ligand field interaction,^{5,8,10,18} the comparison of ^{195}Pt -NMR data for **5a** ($\delta = -4260 \text{ ppm}$), $[\text{Pt}\{[(\eta^5\text{-C}_5\text{H}_3)\text{-CH=N-(CH}_2\text{-CH}_2\text{)-NMe}_2]\}\text{Fe}(\eta^5\text{-C}_5\text{H}_5)\text{Cl}(\text{PPh}_3)]$ (**5c**) ($\delta = -4197 \text{ ppm}$ ^{8a}) and **5b** ($\delta = -4180 \text{ ppm}$) suggests that the strength of the interaction between the $\text{Pt}(\text{II})$ and the bidentate $(\text{C},\text{N})^-$ ligands increases according to the sequence: **5b** < **5c** < **5a**.

The UV-vis spectra of $5 \times 10^{-5} \text{ M}$ solutions of the ligand (**1b**) and compounds **2b-5b** were registered in CH_2Cl_2 at 298 K (Fig. 4 and Table 2). A summary of the results obtained from these studies is presented in Table 2.

All spectra (Fig. 4) showed three bands. According to previous studies on UV-vis spectra of $[(\eta^5\text{-C}_5\text{H}_5)\text{Fe}\{(\eta^5\text{-C}_5\text{H}_4)\text{-CH=N-(R}^2)\}]$ the two bands in the range $300 \text{ nm} < \lambda < 480 \text{ nm}$ are attributed to intraligand transitions

[§] Due to the low stability of compounds **6b** and **7b** in CDCl_3 and acetonitrile- d_3 , their $^{195}\text{Pt}\{^1\text{H}\}$ -NMR spectrum was not registered.

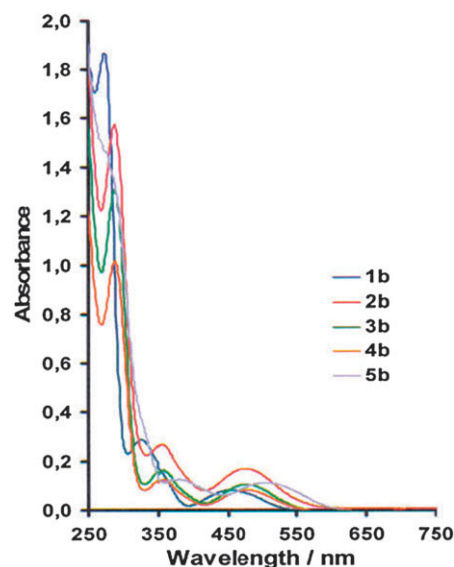


Fig. 4 UV-vis spectra of $5 \times 10^{-5} \text{ M}$ solutions of the free ligand (**1b**), the two isomers of $[\text{Pt}\{(\eta^5\text{-C}_5\text{H}_5)\text{Fe}(\eta^5\text{-C}_5\text{H}_4)\text{-CH=N-(CH}_2\text{-CH}_2\text{-OH)}\}]\text{Cl}_2(\text{dmsol})$ $\{trans\text{-}(\mathbf{2b}) \text{ and } cis\text{-}(\mathbf{3b})\}$ and the platinumacycles $[\text{Pt}\{[(\eta^5\text{-C}_5\text{H}_3)\text{-CH=N-(CH}_2\text{-CH}_2\text{-OH)}]\text{Fe}(\eta^5\text{-C}_5\text{H}_5)\}\text{Cl}(\text{L})]$ $\{with \text{ L} = \text{dmsol } (\mathbf{4b}) \text{ or } \text{PPh}_3 (\mathbf{5b})\}$ in CH_2Cl_2 at 298 K.

Table 2 Summary of the experimental UV-vis spectroscopic data for $[(\eta^5\text{-C}_5\text{H}_5)\text{Fe}\{(\eta^5\text{-C}_5\text{H}_4)\text{-CH=N-(CH}_2\text{-CH}_2\text{-OH)}\}]$ (**1b**) and its platinum(II) derivatives (**2b-5b**) in CH_2Cl_2 at 298 K: wavelengths (λ_i in nm) and molar extinction coefficients $\{\epsilon_i$ in $\text{mol}^{-1} \text{ dm}^2$ (in parentheses) $\}$

Compound	$\lambda_1(\epsilon_1)$	$\lambda_2(\epsilon_2)$	$\lambda_3(\epsilon_3)$
1b	273(37 400)	325(5040)	453(3240)
2b	287(31 600)	355(5320)	473(3800)
3b	287(25 200)	358(5180)	481(3300)
4b	283(22 400)	368(4260)	518(3860)
5b	290(28 800) ^a	378(3140)	505(3019)

^a Shoulder.

(ILT) $[3d(\text{Fe}) \rightarrow \pi^*$ and $\pi \rightarrow \pi^*$, respectively].^{10,11b} For the platinum(II) complexes these bands, that are due to metal perturbed intraligand transitions (MPILT), appeared at lower energies than for the free ligand (**1b**). For the platinumacycles (**4b** and **5b**) the magnitude of the shift is greater than for **2b** and **3b**. This trend is similar to that found for compounds **1a-6a**.^{5b}

Furthermore, comparison of UV-vis data for the two families of compounds (**2a-6a** and **2b-6b**)^{5b} reveals that the replacement of the R^1 moiety in **2a-6a** ($\text{R}^1 = 1,2\text{-C}_6\text{H}_4$) by the $\text{-CH}_2\text{-CH}_2\text{-}$ unit produces a shift (of *ca.* 15–20 nm) of the absorption maxima of the two MPILT to higher energies. This suggests that the R^1 unit modifies the energy of the $3d(\text{Fe})$, π and π^* levels involved in these transitions. Molecular orbital (MO) calculations of **1a**¹⁹ and of metallacycles derived from $[(\eta^5\text{-C}_5\text{H}_5)\text{Fe}\{(\eta^5\text{-C}_5\text{H}_4)\text{-CH=N-R}^2\}]$ (with $\text{R}^2 = \text{other substituted phenyl groups}$) have shown that the HOMO and LUMO are not solely iron based. In these MO there is a contribution of π^* orbitals of the phenyl unit on the imine nitrogen.^{10,11b,19} However, this is not possible in compounds with $\text{R}^1 = \text{-CH}_2\text{-CH}_2\text{-}$.

Description of the crystal structures of **4b** and **5b**

These structures consist of molecules of $[\text{Pt}\{[(\eta^5\text{-C}_5\text{H}_5)\text{-CH=N-(CH}_2\text{-CH}_2\text{-OH)]Fe}(\eta^5\text{-C}_5\text{H}_5)\}\text{Cl(L)}]$ $\{\text{L} = \text{dmsO}$ (for **4b**) or PPh_3 (for **5b**) $\}$. ORTEP plots are shown in Fig. 5 and 6. In the two cases, bond lengths and angles around the platinum (II) atom are similar to those reported for related platinumacycles of the type $[\text{Pt}\{\kappa^2\text{-C}(\text{sp}^2, \text{ferrocene}), \text{N-ligand}\}\text{Cl(L)}]$ with $\text{L} = \text{dmsO}$ or PPh_3 .^{5b,20} The values of the bond angles C(6)-Pt-S $\{95.88(5)^\circ$ (in **4b**) $\}$ and C(6)-Pt-P(1) $\{92.5(3)^\circ$ (in **5b**) $\}$ indicate that the neutral ligands L are in a *cis*-arrangement to the metallated carbon, in good agreement with the transphobia effect.¹⁵

Each one of the molecules of $[\text{Pt}\{[(\eta^5\text{-C}_5\text{H}_5)\text{-CH=N-(CH}_2\text{-CH}_2\text{-OH)]Fe}(\eta^5\text{-C}_5\text{H}_5)\}\text{Cl(L)}]$ contains a [5.5] bicyclic system formed by a five-membered platinumacycle and the substituted ring of the ferrocenyl unit. In **4b** and **5b** the set of atoms that define the platinumacycle $[\text{Pt}, \text{N(1)}, \text{C(6)}, \text{C(10)}, \text{C(11)}]$, are nearly co-planar (the puckering analyses gives τ values of 3.0 and 4.3, respectively).

In each molecule of $[\text{Pt}\{[(\eta^5\text{-C}_5\text{H}_5)\text{-CH=N-(CH}_2\text{-CH}_2\text{-OH)]Fe}(\eta^5\text{-C}_5\text{H}_5)\}\text{Cl(L)}]$ the platinum atom is located in a slightly distorted square-planar environment and it is bound to the imine nitrogen, N(1) and the C(6) carbon atom of the ferrocenyl unit. Thus, confirming that the mode of binding of **1b** is $[\text{C}(\text{sp}^2, \text{ferrocene}), \text{N}]^-$. One chloride and the sulfur atom of the dmsO ligand (in **4b**) or the phosphorous of the PPh_3 ligand (in **5b**) fulfil the coordination sphere.

In the molecules of $[\text{Pt}\{[(\eta^5\text{-C}_5\text{H}_5)\text{-CH=N-(CH}_2\text{-CH}_2\text{-OH)]Fe}(\eta^5\text{-C}_5\text{H}_5)\}\text{Cl(L)}]$ $\{\text{L} = \text{dmsO}$ (**4b**) or PPh_3 (**5b**) $\}$, the oxygen atom of the -OH unit is out of the coordination plane and it is close to the C_5H_5 moiety. The separation between the O(1) atom and the hydrogen atom: H(5) in **4b** or H(1) in **5b**, being: 3.06 Å and 2.74 Å, respectively.

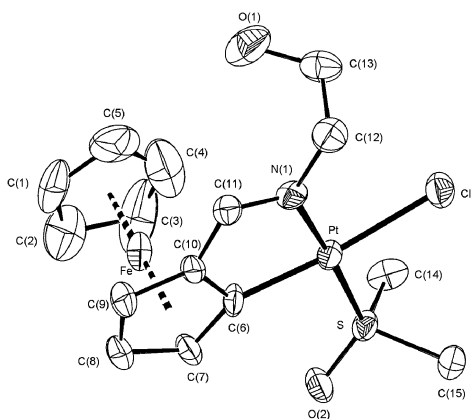


Fig. 5 ORTEP plot (50% probability thermal ellipsoids) of $[\text{Pt}\{[(\eta^5\text{-C}_5\text{H}_5)\text{-CH=N-(CH}_2\text{-CH}_2\text{-OH)]Fe}(\eta^5\text{-C}_5\text{H}_5)\}\text{Cl(dmsO)}]$ (**4b**). Hydrogen atoms have been omitted for clarity. Selected bond lengths (in Å) and bond angles (in $^\circ$): Pt-C(6) , 2.016(5); Pt-N(1) , 2.078(4); Pt-Cl , 2.3947(19); Pt-S , 2.1977(16); C(6)-C(10) , 1.427(7); C(10)-C(11) , 1.417(7); C(11)-N(1) , 1.298(7); N(1)-C(12) , 1.454(8); C(12)-C(13) , 1.483(11); C(13)-O(1) , 1.444(10); C(6)-Pt-N(1) , 80.5(2); N(1)-Pt-Cl , 93.21(15); Cl-Pt-S , 90.45(6); C(6)-Pt-S , 95.88(15); Pt-C(6)-C(10) , 112.0(4); C(6)-C(10)-C(11) , 115.8(5); C(10)-C(11)-N(1) , 117.7(4); C(11)-N(1)-Pt , 113.8(3) and C(12)-N(1)-Pt , 125.8(4).

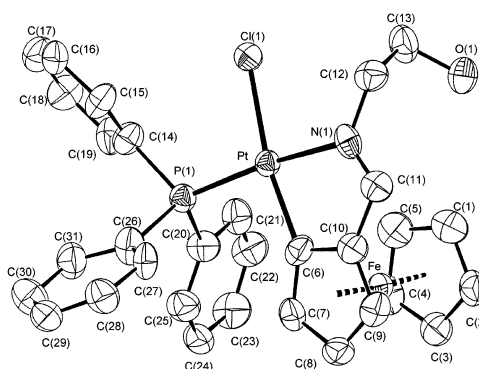


Fig. 6 ORTEP plot (50% probability thermal ellipsoids) of $[\text{Pt}\{[(\eta^5\text{-C}_5\text{H}_5)\text{-CH=N-(CH}_2\text{-CH}_2\text{-OH)]Fe}(\eta^5\text{-C}_5\text{H}_5)\}\text{Cl(PPh}_3)]$ (**5b**). Hydrogen atoms have been omitted for clarity. Selected bond lengths (in Å) and bond angles (in $^\circ$): Pt-C(6) , 2.026(9); Pt-N(1) , 2.190(7); Pt-Cl(1) , 2.376(2); Pt-P(1) , 2.243(3); C(6)-C(10) , 1.483(11); C(10)-C(11) , 1.509(12); C(11)-N(1) , 2.56(10); N(1)-C(12) , 1.544(12); C(12)-C(13) , 1.592(12); C(13)-O(1) , 1.440(10); C(6)-Pt-N(1) , 80.7(3); N(1)-Pt-Cl(1) , 92.0(2); Cl(1)-Pt-P(1) , 95.36(9); C(6)-Pt-P(1) , 92.5(3); Pt-C(6)-C(10) , 110.1(7); C(6)-C(10)-C(11) , 119.1(8); C(10)-C(11)-N(1) , 113.4(8); C(11)-N(1)-Pt , 116.4(7) and C(12)-N(1)-Pt , 126.0(6).

Bond lengths and angles of the ferrocenyl moiety agree with the values reported for other 1,2-disubstituted ferrocene derivatives.²⁰ The two pentagonal rings are planar, nearly parallel [tilt angles = 2.3° (for **4b**) and 1.7° (for **5b**)], and they deviate by *ca.* 10.6° (in **4b**) and 0.5° (in **5b**) from the ideal eclipsed conformation. The separation between the Pt(II) and the Fe(II) atoms $[3.587 \text{ \AA}$ (for **4b**) and 3.621 \AA (for **5b**)] clearly exceeds the sum of the van der Waals radii²¹ of these atoms, thus precluding the existence of any direct interaction.

In the crystals of **4b** and **5b**, there are weak intermolecular $\text{Cl} \cdots \text{H-O}$ interactions connecting two molecules of $[\text{Pt}\{[(\eta^5\text{-C}_5\text{H}_5)\text{-CH=N-(CH}_2\text{-CH}_2\text{-OH)]Fe}(\eta^5\text{-C}_5\text{H}_5)\}\text{Cl(L)}]$ $\{\text{L} = \text{dmsO}$ (in **4b**) or PPh_3 (in **5b**) $\}$ (Fig. 7).

Electrochemical studies

In order to elucidate the effect induced by: (a) the mode of binding of the ligand, (b) the relative arrangement of the Cl^- ligands in **2b** and **3b**, and the nature of R^1 in the platinum(II) complexes with $\text{R}^1 = \text{-CH}_2\text{-CH}_2\text{-}$ (in **2b-5b**) or 1,2- C_6H_4 (**2a-5a**) on the electronic environment of the Fe(II) , we also undertook electrochemical studies of compounds **2b-5b** based on cyclic voltammograms.¶ As shown in Fig. 8 the cyclic voltammograms exhibit an anodic peak with a directly associated reduction peak in the reverse scan.

A summary of the most relevant electrochemical parameters is presented in Table 3 together with those reported for compounds **2a-5a** under identical experimental conditions. For compounds under study the ΔE values depart appreciably

¶ $^1\text{H-NMR}$ spectra of **2b-5b** in acetonitrile- d_3 (see Experimental) indicate that these products are stable in this solvent. In the $^1\text{H-NMR}$ spectrum of **6b** in CD_3CN the signals were broader than expected and its $^{31}\text{P}\{^1\text{H}\}$ -NMR spectrum showed two singlets at 17.3 ($^1J_{\text{P-Pt}} = 4098 \text{ Hz}$) and at 16.7 ppm ($^1J_{\text{P-Pt}} = 3425 \text{ Hz}$) {of relative intensities 1.0:0.2}, respectively that correspond to **5b** and **6b**, respectively.

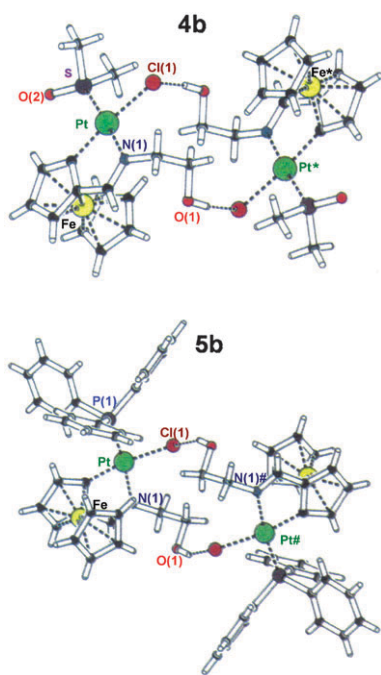


Fig. 7 Schematic view of the intermolecular Cl...H-O interactions between molecules of $[\text{Pt}\{[(\eta^5\text{-C}_5\text{H}_5)\text{-CH=N-(CH}_2\text{-CH}_2\text{-OH)]-Fe}(\eta^5\text{-C}_5\text{H}_5)\}\text{Cl(L)}]$ in the crystals of **4b** (L = dmsO) and **5b** (L = PPh_3).

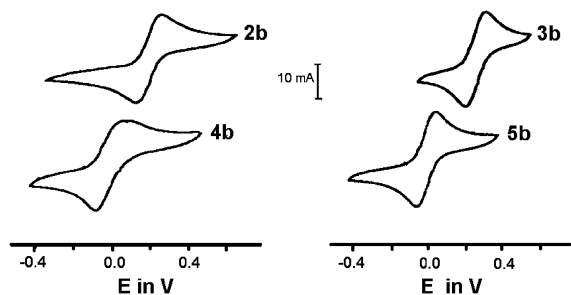


Fig. 8 Cyclic voltammograms of the isomers of $[\text{Pt}\{[(\eta^5\text{-C}_5\text{H}_5)\text{Fe}\{(\eta^5\text{-C}_5\text{H}_4)\text{-CH=N-(CH}_2\text{-CH}_2\text{-OH)}\}]\text{Cl}_2(\text{dmsO})\}]$ $\{trans\text{-}(\mathbf{2b})$ and $cis\text{-}(\mathbf{3b})\}$ and the platinacycles $\{L = \text{dmsO} (\mathbf{4b})$ or $\text{PPh}_3 (\mathbf{5b})\}$ in CH_3CN at 298 K and $\nu = 100 \text{ mV s}^{-1}$.

Table 3 Summary of electrochemical data $\{$ anodic (E_{pa}) and cathodic (E_{pc}) potentials and separation between peaks (ΔE) in mV $\}^a$ at a scan speed $\nu = 100 \text{ mV s}^{-1}$ for $[(\eta^5\text{-C}_5\text{H}_5)\text{Fe}\{(\eta^5\text{-C}_5\text{H}_4)\text{-CH=N-(CH}_2\text{-CH}_2\text{-OH)}\}]\text{Cl}_2(\text{dmsO})$ (**1b**) and its platinum(II) derivatives (**2b–5b**). For comparison purposes data for $[(\eta^5\text{-C}_5\text{H}_5)\text{Fe}\{(\eta^5\text{-C}_5\text{H}_4)\text{-CH=N-(C}_6\text{H}_4\text{-2-OH)}\}]\text{Cl}_2(\text{dmsO})$ (**1a**), the isomers of $[\text{Pt}\{(\eta^5\text{-C}_5\text{H}_5)\text{Fe}\{(\eta^5\text{-C}_5\text{H}_4)\text{-CH=N-(C}_6\text{H}_4\text{-2-OH)}\}]\text{Cl}_2(\text{dmsO})$ $\{trans\text{-}(\mathbf{2a})$ and $cis\text{-}(\mathbf{3a})\}$ and the platinacycles $[\text{Pt}\{[(\eta^5\text{-C}_5\text{H}_5)\text{-CH=N-(C}_6\text{H}_4\text{-2-OH)}]\text{Fe}(\eta^5\text{-C}_5\text{H}_5)\}\text{Cl(L)}]$ $\{$ with L = dmsO (**4a**) or PPh_3 (**5a**) $\}$ are also enclosed^b

	E_{pa}	E_{pc}	ΔE		E_{pa}	E_{pc}	ΔE
1b ^c	98	30	68	1a	258	178	80
2b	262	106	156	2a	415	294	121
3b	299	181	118	3a	474	323	151
4b	74	-98	162	4a	116	15	101
5b	51	-74	125	5a	151	-3	155

^a In all cases the E_{pa} and E_{pc} values are referenced to the ferrocene/ferrocinium couple. ^b Data for **1a–5a** were taken from ref. 5b. ^c Data from ref. 6.

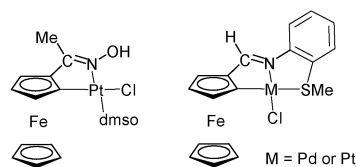


Fig. 9 Cyclometallated compounds: $[\text{Pt}\{[(\eta^5\text{-C}_5\text{H}_5)\text{-C(Me)=N-OH)]-Fe}(\eta^5\text{-C}_5\text{H}_5)\}\text{Cl(dmsO)}]$ and $[\text{M}\{[(\eta^5\text{-C}_5\text{H}_5)\text{-CH=N-(C}_6\text{H}_4\text{-2-SMe)]-Fe}(\eta^5\text{-C}_5\text{H}_5)\}\text{Cl}]$ with M = Pd or Pt described before.^{10,24}

from the constant value of 59 mV (theoretically expected for an electrochemically reversible one-electron-step oxidation-reduction process) suggesting that a structural reorganization takes place upon oxidation.²²

The cyclic voltammograms of the *trans*-(**2b**) and *cis*-(**3b**) isomers of $[\text{Pt}\{(\eta^5\text{-C}_5\text{H}_5)\text{Fe}\{(\eta^5\text{-C}_5\text{H}_4)\text{-CH=N-(CH}_2\text{-CH}_2\text{-OH)}\}]\text{Cl}_2(\text{dmsO})]$ were similar to that of the free ligand (**1b**) except for the position of the wave that appeared strongly shifted to more anodic potentials and this suggests that the binding of the platinum(II) to **1b** inhibits the oxidation of the ferrocenyl unit. This trend is similar to that reported for **1a** compounds **2a**, **3a**, the imines $[(\eta^5\text{-C}_5\text{H}_5)\text{Fe}\{(\eta^5\text{-C}_5\text{H}_4)\text{-C(R}^1\text{)=N-R}^2\}]$ ($\text{R}^1 = \text{H, Me or Ph}$ and $\text{R}^2 = \text{phenyl or benzyl}$ groups) and their platinum(II) or palladium(II) derivatives where these ligands act as an N-donor group.^{5b,11b,23}

For the platinacycles $[\text{Pt}\{[(\eta^5\text{-C}_5\text{H}_5)\text{-CH=N-(CH}_2\text{-CH}_2\text{-OH)]Fe}(\eta^5\text{-C}_5\text{H}_5)\}\text{Cl(L)}]$ $\{$ with L = dmsO (**4b**) or PPh_3 (**5b**) $\}$ the ferrocene-centred transition shifts to more cathodic potentials. This agrees with the results reported for $[\text{Pt}\{[(\eta^5\text{-C}_5\text{H}_5)\text{-C(Me)=NOH)]Fe}(\eta^5\text{-C}_5\text{H}_5)\}\text{Cl(dmsO)}]$ ²⁴ or $[\text{M}\{[(\eta^5\text{-C}_5\text{H}_5)\text{-CH=N-(C}_6\text{H}_4\text{-2-SMe)]Fe}(\eta^5\text{-C}_5\text{H}_5)\}\text{Cl}]$ (M = Pd or Pt)¹⁰ and their corresponding free ligands (Fig. 9).

Conclusions

The studies presented here have allowed us: (a) to compare the reactivity of the ferrocenyl Schiff bases $[(\eta^5\text{-C}_5\text{H}_5)\text{Fe}\{(\eta^5\text{-C}_5\text{H}_4)\text{-CH=N-(R}^1\text{)-OH}\}]$ $\{$ with $\text{R}^1 = 1,2\text{-C}_6\text{H}_4$ (**1a**) or $\text{-CH}_2\text{-CH}_2\text{-}$ (**1b**) $\}$ with respect to *cis*- $[\text{PtCl}_2(\text{dmsO})_2]$ and (b) to demonstrate the relevancy of the nature of the R^1 moiety on these processes and the properties of the final products.

Ligands **1a** and **1b** exhibit a similar behaviour in refluxing methanol giving $[\text{trans-}(\mathbf{2a}, \mathbf{2b})$ or $cis\text{-}(\mathbf{3a}, \mathbf{3b})]$ isomers of $[\text{Pt}\{(\eta^5\text{-C}_5\text{H}_5)\text{Fe}\{(\eta^5\text{-C}_5\text{H}_4)\text{-CH=N-(R}^1\text{)-OH}\}]\text{Cl}_2(\text{dmsO})]$. However, in the presence of a two-fold excess of NaAcO and using a toluene-MeOH (5 : 1) mixture as solvent, the final products (**7a** and **4b**, respectively) are markedly different. Compounds **1a** and **1b** contain an acidic -OH functionality,²⁴ but in **7a** the ligand behaves as a terdentate $[\text{C}(\text{sp}^2, \text{ferrocene}), \text{N}, \text{O}]^2-$ group; while in **4b**, the aldimine **1a** acts as bidentate $[\text{C}(\text{sp}^2, \text{ferrocene}), \text{N}]^-$ ligand.

The crystal structure of **1a**¹⁹ shows that the oxygen atom of the -OH group it is nearly coplanar with the imine unit and close to the imine nitrogen; while in **1b**,⁶ where the R^1 unit is more flexible, the location of the -OH moiety is similar to those of **4b** and **5b**. This suggests that once the Pt(II) ion binds to the nitrogen of **1a** or **1b**, the oxygen atom of **1a** would be closer to the metal centre than for **1b**. In the presence of

AcO⁻ the two ligands (**1a** and **1b**) undergo the formation of the platinacycles with a $\sigma\{\text{Pt}-\text{C}(\text{sp}^2, \text{ferrocene})\}$ bond. For **1a** the acidic -OH group²⁵ is closer to the Pt(II) centre than in **1b**, and the AcO⁻, also allows the deprotonation of the -OH unit and the formation of the Pt-O bond giving **7a** with a [C(sp², ferrocene), N, O]²⁻ ligand. A similar argument can be used to explain why **4b** and **5b** are less prone to form complexes with terdentate [C(sp², ferrocene), N, O]²⁻ ligands than their analogues with R¹ = 1,2-C₆H₄ (**4a** and **5a**).

Furthermore, the comparison of the electrochemical properties of ligands (**1a** and **1b**) and those of their platinum(II) complexes (**2a-5a** and **2b-5b**) has also shown that the replacement of the 1,2-C₆H₄ unit (in **1a**) by the -CH₂-CH₂- moiety (in **1b**) increases the proclivity of the ferrocenyl unit to undergo oxidation. In general, **2b-5b** are more prone to oxidize than their analogues with R¹ = 1,2-C₆H₄ (**2a-5a**).

It has been reported that [Pt{[(η⁵-C₅H₅)-CH₂-NMe₂]-Fe(η⁵-C₅H₅)}Cl(dmsO)], (where the environment of the Pt(II) is very similar to that of **4b**) exhibits antitumour activity,²⁶ and consequently, the platinacycle **4b** appears to be an excellent candidate for future studies in this area.

On the other hand, we have also shown that in **6b** and **7b** the Pt-O bond is more labile than in their analogues with R¹ = 1,2-C₆H₄ (**6a** and **7a**). Unfortunately, this reduces the potential utility of the pairs of products (**5b** and **6b**) and (**4b** and **7b**) as molecular switches, but it can be potentially interesting for the design of pH-dependent devices. Mainly due to the extracellular acidity of solid tumors at present there is an increasing interest in the design of pH-activable compounds for diagnostic and/or therapeutic aims.²⁷ Several examples of platinum(II) complexes exhibiting higher cytotoxic activity with decreasing pH have been reported.²⁸ Thus, the lability of the Pt-O bond in **6b** or **7b** makes them specially attractive from this point of view. Further work on this field is currently under study.

Experimental

Materials and methods

Compounds **1b**, **2b** and *cis*-[PtCl₂(dmsO)₂] were prepared as reported previously^{6,7} and the remaining reagents were obtained from commercial sources and used as received. Except methanol, that was HPLC-grade, the remaining solvents used were dried and distilled before use.²⁹ Elemental analyses were carried out at the Serveis de Científico-Tècnics (Universitat Barcelona). Mass spectra (ESI⁺) were performed at the Servei d'Espectrometria de Masses (Universitat de Barcelona). Infrared spectra were obtained with a Nicolet 400FTIR instrument using KBr pellets. UV-visible spectra of 5 × 10⁻⁵ M solutions of compounds **1b-5b** in CH₂Cl₂ were registered with a Cary-100 scan Varian-UV spectrometer at 298 K. Routine ¹H and ¹³C{¹H}-NMR spectra were recorded with a Mercury-400 MHz instrument. High resolution ¹H-NMR spectra and the two-dimensional [{¹H-¹H}-NOESY and COSY and {¹H-¹³C}-HSQC and HMBC] experiments were registered with a Varian VRX-500 or a Bruker Avance DMX-500 MHz instruments at 298 K. The chemical shifts (δ) are given in ppm and the coupling

constants (*J*) in Hz. ¹⁹⁵Pt{¹H}-NMR spectra of **4b** and **5b** were obtained with a Bruker-250 MHz instrument at 298 K. ³¹P{¹H}-NMR spectra of **5b** and **6b** were recorded with a Varian-Unity-300 instrument. In all cases the solvent for the NMR experiments was CDCl₃ (99.9%) and the references were SiMe₄ [for ¹H and ¹³C{¹H}-NMR], P(OMe)₃ [δ(³¹P) = 140.17 ppm, for ³¹P{¹H}-NMR] and H₂[PtCl₆] [for ¹⁹⁵Pt{¹H}-NMR]. In order to test the stability of the platinum(II) compounds in the solvent used for electrochemical studies the ¹H-NMR spectra of these products in acetonitrile-*d*₃ (99.8%) were also registered at 298 K.

Some of the preparations described below required the use of highly hazardous reagents such as benzene that should be handled with *caution*!

Preparation of the compounds

Cis-[Pt{(η⁵-C₅H₅)Fe(η⁵-C₅H₄)-CH=N-(CH₂-CH₂-OH)}]-Cl₂ (dmsO) (**3b**). *Cis*-[PtCl₂(dmsO)₂] (211 mg, 5.0 × 10⁻⁴ mol) was suspended in 40 mL of MeOH. The reaction flask was protected from the light with aluminium foil and refluxed until complete dissolution and then it was filtered. Afterwards, an equimolar amount of ligand **1b** (129 mg, 5.0 × 10⁻⁴ mol) was added to the filtrate and the resulting solution was refluxed for 20 h. After this period the solution was filtered and concentrated to dryness on a rotary evaporator. The deep-brown residue obtained was dried in vacuum for one night and afterwards it (260 mg) was treated with 15 mL of a CHCl₃:acetone (8:1) mixture and passed through a (2.0 cm × 2.5 cm) SiO₂ column using the same CHCl₃:acetone solution as eluant. This produced the release of two bands. The first eluted one gave, after concentration to dryness, **3b** (191 mg) as a red microcrystalline product. The next band released was collected and concentrated to dryness giving complex **2b** (68 mg) as an orange powder. *Characterization data*: Anal. calc. for C₁₅H₂₁Cl₂FeNO₂PtS: C, 29.97; H, 3.52; N, 2.33; S, 5.33%; found: C, 30.1; H, 3.6; N, 2.4; S, 5.5%. EM(ESI⁺): *m/z* = 566.0 {[M] - Cl}⁺, 623.9 {[M] + Na}⁺, 1225.0 {2[M] + Na}⁺ and 1229 {2[M] + NH₄}⁺. IR data: 1625 {ν(>C=N-)} and 3450 cm⁻¹ {ν(O-H)}. ¹H-NMR data in CDCl₃:|| 8.23 (s, 1H, ³J_{H-Pt} = 88 -CH=N-), 4.42 (s, 5H, C₅H₅), 4.83 (s, 1H, H²), 4.70 (s, 1H, H³), 4.73 (s, 1H, H⁴), 6.92 (s, 1H, H⁵), 3.70 (br m, 1H, -OH), 4.25-4.27 (m, 2H, =N-CH₂-), 3.25-3.47 (m, 2H, -CH₂-), 3.47 [s, 3H, J_{Pt-H} = 18, Me(dmsO)] and 3.25 [s, 3H, ³J_{Pt-H} = 19, Me(dmsO)]. ¹H-NMR data in acetonitrile-*d*₃:|| 8.46 (s, 1H, ³J_{H-Pt} = 95, -CH=N-), 4.44 (s, 5H, C₅H₅), 5.05 (s, 1H, H²), 4.90 (s, 1H, H³), 4.82 (s, 1H, H⁴), 6.59 (s, 1H, H⁵), 3.80 (br.m, 1H, -OH), 4.205-4.30 (m, 2H, =N-CH₂-), 3.28-3.67 (m, 2H, -CH₂-), 3.42 [s, 3H, J_{Pt-H} = 19, Me(dmsO)] and 3.39 [s, 3H, ³J_{Pt-H} = 18, Me(dmsO)]. ¹³C{¹H}-NMR data in CDCl₃:|| 171.7 (-CH=N-), 75.1 (C¹), 74.5 (C²), 73.3 (C³), 74.2 (C⁴), 75.9 (C⁵), 70.9 (C₅H₅), 45.1 and 45.0 [Me(dmsO)], 60.3 (-CH₂-), 69.6 (=N-CH₂-). ¹⁹⁵Pt{¹H}-NMR data: -2942.

[Pt{(η⁵-C₅H₅)-CH=N-(CH₂-CH₂-OH)Fe(η⁵-C₅H₅)}Cl (dmsO) (**4b**). This compound can be obtained using two

|| Numbering of the atoms refers to that shown in Scheme 1; abbreviations: s = singlet, d = doublet, t = triplet, m = multiplet, br = broad.

alternative procedures {methods (a) and (b), respectively} that differ in the nature of the starting material. The procedure described in method (a) allows the isolation of **4b** in a high yield and its separation is easier.

Method (a): Ligand **1b** (129 mg, 5.0×10^{-4} mol), *cis*-[PtCl₂(dmsO)₂] (211 mg, 5.0×10^{-4} mol) were dissolved in 50 mL of toluene. Then, a solution formed by 10.0×10^{-4} mol (41 mg) of NaAcO and 10 mL of MeOH was added. The reaction mixture was protected from the light with aluminium foil and refluxed for 120 h. After this period the hot solution was filtered, and the filtrate was concentrated to dryness on a rotary evaporator. The residue was then treated with the minimum amount of CH₂Cl₂ and passed through a SiO₂ column (2.5 cm × 4.0 cm). Elution with CH₂Cl₂ produced the release of three orange bands that gave, after concentration, FeCHO (10 mg), **2b** (9 mg) and **3b** (24 mg), respectively. Once these bands were collected a garnet one was released, and the evaporation of the solvent produced **4b** (163 mg) that was collected, and dried in vacuum for two days.

Method (b): Compound **2b** (300 mg, 5.0×10^{-4} mol) was dissolved in 30 mL of methanol, then a solution containing an equimolar amount of NaAcO in MeOH (5 mL) was added. The reaction mixture was protected from the light with aluminium foil and refluxed for 120 h. After this period, the solution was filtered and the filtrate was concentrated to dryness on a rotary evaporator. The deep-brown residue was then dissolved in the minimum amount of CH₂Cl₂ and passed through a SiO₂ column (2.5 cm × 4.0 cm). The elution with CH₂Cl₂ produced the release of two pale orange bands. The first eluted one gave after concentration, traces (9 mg) of FeCHO and the second one produced, after work up, **3b** (46 mg). Concentration to dryness of the garnet band released afterwards gave **4b** that was collected and dried in vacuum for two days (138 mg).

Characterization data. Anal. calc. for C₁₅H₂₀ClFeNO₂PtS: C, 31.90; H, 3.57; N, 2.48; S, 5.68%; found: C, 32.05; H, 3.6; N, 2.5; S, 5.8%. EM(ESI⁺): *m/z* = 564.0 [M]⁺ and 528.5 {[M] – Cl}⁺. IR data: 1597 {ν(>C=N–)} and 3408 cm⁻¹ {ν(O–H)}. ¹H-NMR data in CDCl₃: || 8.10 (s, 1H, ³J_{H–Pt} = 103, –CH=N–), 4.21 (s, 5H, C₅H₅), 4.37 (t, 1H, ³J = 1.5, H³), 4.50 (d, 1H, *J* = 1.5, H⁴), 4.58 (t, 1H, ³J = 1.5, H⁵), 4.2 (br m, 1H, –OH), 4.17–4.22 (br.m, 2H, =N–CH₂–), 3.88 and 3.93 (m, 2H, –CH₂–), 3.53 [s, 3H, ³J_{Pt–H} = 25, Me(dmsO)] and 3.57 [s, 3H, ³J_{Pt–H} = 21, Me(dmsO)]. ¹H-NMR data in acetonitrile-*d*₃: || 8.25 (s, 1H, ³J_{H–Pt} = 98, –CH = N–), 4.35 (s, 5H, C₅H₅), 4.42 (t, 1H, ³J = 1.5 H³), 4.63 (d, 1H, ³J = 1.5, H⁴), 4.49 (t, 1H, ³J = 1.5, H⁵), 4.10–4.29 (br.m, 2H, =N–CH₂–), 3.50 and 3.70 (br m, 3H, –CH₂– and –OH), 3.49 [s, 3H, ³J_{Pt–H} = 22, Me(dmsO)] and 3.46 [s, 3H, ³J_{Pt–H} = 20, Me(dmsO)]. ¹³C{¹H}-NMR data in CDCl₃: || 179.2(–CH=N–), 70.5 (C₅H₅), 84.2 (C¹), 101.4 (C²), 72.1 (C³), 73.9 (C⁴), 74.8 (C⁵), 64.3 (=N–CH₂–), 59.4 (–CH₂–), 47.1 and 46.9 [Me(dmsO)]. ¹⁹⁵Pt{¹H} NMR data in CDCl₃: –3791 ppm.

[Pt{(η⁵-C₅H₅)-CH=N-(CH₂-CH₂-OH)Fe(η⁵-C₅H₅)}Cl (PPh₃)] (**5b**). Compound **4b** (30 mg, 5.3×10^{-5} mol) was dissolved in 10 mL of benzene, then 14 mg (5.3×10^{-5} mol) of PPh₃ were added. The reaction mixture was heated at 70 °C

for 1.5 h. Then, the hot solution was filtered and the undissolved material was discarded. The filtrate was concentrated to dryness on a rotary evaporator and the deep-red residue was then dissolved in the minimum amount of CH₂Cl₂ and passed through a small (1.5 cm × 2.0 cm) SiO₂ column to remove the free dmsO. Elution with CH₂Cl₂ produced the release of a purple band that was collected and concentrated to dryness on a rotary evaporator. The solid formed was air-dried and then dried in vacuum for 3 days (Yield: 31 mg, 77.5%). *Characterization data:* Anal. calc. for C₃₁H₂₉ClFeNOPPt: C, 49.72; H, 3.90; N, 1.87%; found: C, 49.8; H, 3.95; N, 1.95%. EM(ESI⁺): *m/z* = 713.1 {[M] – Cl}⁺. IR data: 1592 {ν(>C=N–)} and 3402 cm⁻¹{ν(O–H)}. ¹H-NMR data in CDCl₃: || 8.25 (s, d, 1H, ³J_{H–Pt} = 88 and ⁴J_{H–P} = 9.0, –CH=N–), 3.93 (s, 5H, C₅H₅), 3.39 (s, 1H, H³), 4.29 (s, 1H, H⁴), 4.49 (s, 1H, H⁵), 4.10 and 4.29 (m, 2H, =N–CH₂–), 3.81 and 3.89 (m, 2H, –CH₂–), 4.21 (br. m, 1H, –OH) and 7.10–7.80 (m, 15H, aromatic protons of the PPh₃ ligand). ¹H-NMR data in acetonitrile-*d*₃: || 8.45 (s, d, 1H, ¹J_{H–Pt} = 79 and ⁴J_{H–P} = 8.5, –CH=N–), 3.58 (s, 5H, C₅H₅), 3.30 (s, 1H, H³), 4.15 (s, 1H, H⁴), 4.60 (s, 1H, H⁵), 3.80 and 3.90 (m, 2H, –N–CH₂–), 3.60–3.75 (m, 2H, –CH₂–), 4.05 (br m, 1H, –OH), and 7.30–7.80 (m, 15H, aromatic protons of the PPh₃ ligand). ¹³C{¹H}-NMR data in CDCl₃: || 176.1 (–CH=N–), 70.7 (C₅H₅), 86.9 (C¹), 99.3 (C²), 68.3 (C³), 71.6 (C⁴), 76.4 (C⁵), 62.5 (=N–CH₂–), 59.8 (–CH₂–) and four additional doublets centred at 128.2, 130.0, 131.3 and 135.1 due to the four types of ¹³C nuclei of the PPh₃ ligand. ³¹P{¹H} NMR data: in CDCl₃ δ = 17.1 (¹J_{P–Pt} = 4017 Hz) and in acetonitrile-*d*₃: 17.3 (¹J_{P–Pt} = 4098 Hz). ¹⁹⁵Pt{¹H} NMR data in CDCl₃: –4180(¹J_{P–Pt} = 4017 Hz).

[Pt{(η⁵-C₅H₅)-CH=N-(CH₂-CH₂-O)Fe(η⁵-C₅H₅)} (PPh₃)] (**6b**). Compound **5b** (83 mg, 1.11×10^{-4} mol) was dissolved in CH₂Cl₂ (≈ 18 mL), then a solution formed by 8 mg (2×10^{-4} mol) of NaOH dissolved in 3 mL of MeOH was added dropwise. Once the addition had finished, the reaction mixture was stirred at 298 K for 30 min. After this period the undissolved materials were removed by filtration and the deep-purple solution was concentrated to dryness on a rotary evaporator. The solid formed was collected and dried in vacuum for 1 day (yield: 65 mg, 85%).

Characterization data. Anal. calc. for C₃₁H₂₈FeNOPPt: C, 52.26; H, 3.96; N, 1.97%; found: C, 52.3; H, 4.05; N, 2.0%. IR data: 1569 cm⁻¹ {ν(>C=N–)}. ¹H-NMR data (in CDCl₃): || 8.16 (s, d, 1H, ¹J_{H–Pt} = 98 and ⁴J_{H–P} = 10.2, –CH=N–), 3.82 (s, 5H, C₅H₅), 3.15 (s, 1H, H³), 4.22 (s, 1H, H⁴), 4.52 (s, 1H, H⁵), 3.88–4.20 (br. m, 4H, =N–CH₂– and –CH₂–) and 7.29–7.90 (m, 15H, aromatic protons of the PPh₃ ligand). ³¹P{¹H} NMR data for a freshly prepared solution in CDCl₃ δ = 16.3 (¹J_{P–Pt} = 3498 Hz) and in acetonitrile-*d*₃: two signals of relative intensities 1.0:0.2 centred at 16.7 ppm (¹J_{P–Pt} = 3425 Hz) and 17.1 ppm (¹J_{P–Pt} = 4098 Hz) were observed of which the later is identical to that of **5b** under identical experimental conditions.

[Pt{(η⁵-C₅H₅)-CH=N-(CH₂-CH₂-O)Fe(η⁵-C₅H₅)} (dmsO)] (**7b**). This product was prepared as described for **6b**, but using 62 mg of **4b** (1.11×10^{-4} mol) as starting material (yield: 49 mg,

Table 4 Crystal data and details of the refinement of the crystal structures of compounds [Pt{[(η^5 -C₅H₅)-CH=N-(CH₂-CH₂-OH)]-Fe(η^5 -C₅H₅)}Cl (L)] {with L = dmsO (**4b**) or PPh₃ (**5b**)}

	4b	5b
Empirical formula	C ₁₅ H ₂₀ ClFeNO ₂ PtS	C ₃₁ H ₂₉ ClFeNOPt
Formula weight	564.77	748.91
T/K	293	293
Wavelength/Å	0.71069	0.71073
Crystal sizes/mm × mm × mm	0.2 × 0.1 × 0.1	0.09 × 0.05 × 0.05
Crystal system	Triclinic	Triclinic
Space group	<i>P</i> 1̄	<i>P</i> 1̄
<i>a</i> /Å	9.841(5)	9.841(8)
<i>b</i> /Å	10.090(4)	11.040(6)
<i>c</i> /Å	10.239(4)	13.762(8)
α /°	82.85(39)	96.46(3)
β /°	61.73(2)	96.67(4)
γ /°	76.85(3)	107.30(4)
<i>V</i> /Å ³	871.8(7)	1400.7(16)
<i>Z</i>	2	2
<i>D</i> _{calc} /Mg m ⁻³	2.152	1.776
Absorption coefficient/mm ⁻¹	9.124	5.683
<i>F</i> (000)	540	732
θ range for data collection	From 2.84 to 29.93	From 2.65 to 32.43
No. of reflections collected	6864	16 100
No. of reflections unique [<i>R</i> _{int}]	3622[0.0648]	8823[0.0691]
Completeness to $\theta = 25.00$ (%)	93.5	93.4
No. of data	3622	8823
No. of parameters	200	334
Goodness of fit on <i>F</i> ²	1.215	0.843
Final <i>R</i> indices [<i>I</i> > 2 σ (<i>I</i>)]	<i>R</i> ₁ = 0.0298 <i>wR</i> ₂ = 0.0867	<i>R</i> ₁ = 0.0611 <i>wR</i> ₂ = 0.1027
Final <i>R</i> indices (all data)	<i>R</i> ₁ = 0.0305 <i>wR</i> ₂ = 0.0872	<i>R</i> ₁ = 0.1426 <i>wR</i> ₂ = 0.1160

84%). *Characterization data*: Anal. calc. for C₁₅H₁₉FeNO₂PtS: C, 34.10; H, 3.62; N, 2.65; S, 6.07% found: C, 33.95; H, 3.7; N, 2.5; and S, 5.95%. IR data: 1575 cm⁻¹ [ν (>C=N-)]. ¹H-NMR data (in CDCl₃): 8.02 (s, 1H, ³*J*_{H-Pt} = 98, -CH=N-), 4.17 (s, 5H, C₅H₅), 4.56 (t, 1H, ³*J* = 1.5 H³), 4.62 (d, 1H, *J* = 1.5, H⁴), 4.90 (t, 1H, ³*J* = 1.5, H⁵), 4.4–4.2 and 4.25–3.80 (2br m, 4H, -CH₂-CH₂-), 3.42 [s, 3H, Me(dmsO)], and 3.38 [s, 3H, Me(dmsO)].

Electrochemical studies. Electrochemical data for the compounds under study were obtained by cyclic voltammetry under nitrogen at 298 K using CH₃CN (HPLC-grade) as solvent, (Bu₄N)[PF₆] (0.1 M) as supporting electrolyte and an M263A potentiostat from EG&G instruments. The measured potentials (*E*) were referenced to an Ag/AgNO₃ (0.1 M in CH₃CN) electrode separated from the solution by a medium-porosity fritted disk. A platinum wire auxiliary electrode was used in conjunction with a platinum disk working Tacussel EDI rotatory electrode (3.14 mm²). Cyclic voltammograms of ferrocene were recorded before and after each sample to ensure the stability of the Ag/AgNO₃ electrode. Cyclic voltammograms of freshly prepared solutions (10⁻³ M) of the samples were run, and average values of the measured potentials were referenced to ferrocene [*E*(*Fc*)] which was used as internal reference. In all the experiments, the cyclic voltammograms were registered using scan speeds varying from *v* = 10 mV s⁻¹ to 100 mV s⁻¹.

Crystallography†. A prismatic crystal of **4b** or **5b** (sizes in Table 4), was selected and mounted on a MAR345

diffractometer with image plate detector. Unit-cell parameters were determined from 5541 reflections (in the range 3° < θ < 31°) for **4b** or from 37 reflections for **5b** and refined by least-squares method. Intensities were collected with a graphite monochromatized Mo-K α radiation.

For **4b** the number of reflections measured in the range 2.84° ≤ θ ≤ 29.93° was 6864 of which 3622 were non-equivalent by symmetry {*R*_{int}(on *I*) = 0.064} and 3449 reflections were assumed as observed applying the condition *I* > 2 σ (*I*). For **5b**, 16 100 reflections were collected in the range 2.65° ≤ θ ≤ 32.43° of which 8823 were non-equivalent by symmetry {*R*_{int}(on *I*) = 0.069} and the number of reflections assumed as observed was 4053. Lorentz-polarization and absorption corrections were made.

The structure was solved by Direct methods, using SHELXS computer program³⁰ and refined by full-matrix least-squares method with the SHELX97 computer program³¹ using 6864 reflections (for **4b**) and 16 100 (for **5b**) (very negative intensities were not assumed). The function minimized was $\sum w||F_o|^2 - |F_c|^2|^2$, where $w = [\sigma^2(I) + (0.0928P)^2 + 4.8976P]^{-1}$ (for **4b**) and $w = [\sigma^2(I) + (0.0201P)^2]^{-1}$ (for **5b**) and $P = (|F_o| + 2|F_c|)^2/3$; *f*, *f'* and *f''* were obtained from the literature.³² All hydrogen atoms were computed and refined using a riding model with an isotropic temperature factor equal to 1.2 times the equivalent temperature factor of the atom to which is linked. The final *R*(on *F*) factor was 0.054 or 0.0611 (for **4b** and **5b**, respectively), *wR*(on |*F*|²) = 0.149 (for **4b**) and 0.1027 (for **5b**) and goodness of fit = 1.214 or 0.843 (for **4b** and **5b**, respectively) for all the observed reflections.

Acknowledgements

We are grateful to the Ministerio de Educación y Ciencia of Spain for financial support (grant: CTQ2009-11501) and Feder funds.

References

- 1 *Comprehensive Organometallic Chemistry-III*, ed. R. B. Crabtree and D. M. P. Mingos, Elsevier, Oxford, UK, 2007, vol. 8, pp. 145–194, 254–276 and 508–538.
- 2 For recent advances in platinacycles with (C, X) (X = N, S or P) ligands: (a) P. Shao, Y. Li and W. Sun, *Organometallics*, 2008, **27**, 2743–2749; (b) B. Ma, P. I. Djurovich, M. Yousufuddin, R. Bau and M. E. Thompson, *J. Phys. Chem. C*, 2008, **112**, 8022–8031; (c) S. Develay and J. A. G. Williams, *Dalton Trans.*, 2008, 4562–4564.
- 3 For reviews on this area: (a) M. Albrecht and G. van Koten, *Angew. Chem., Int. Ed.*, 2001, **40**, 3750–3781; (b) H. Nishiyama, *Chem. Soc. Rev.*, 2007, **36**, 1133–1141.
- 4 (a) *Ferrocenes. Homogeneous Catalysis, Organic Synthesis. Materials Science*, ed. A. Togni and T. Hayashi, VCH, Weinheim (Germany), 1995; (b) *Ferrocene. Ligands, Materials and Biomolecules*, ed. P. Stepnicka, Wiley, Weinheim (Germany), 2008.
- 5 (a) C. López, A. Caubet, S. Pérez, X. Solans and M. Font-Bardía, *Eur. J. Inorg. Chem.*, 2006, 3974–3984; (b) S. Pérez, C. López, A. Caubet, R. Bosque, X. Solans and M. Font-Bardía, *Eur. J. Inorg. Chem.*, 2008, 1599–1612.
- 6 C. López, A. Caubet, X. Solans and M. Font-Bardía, *J. Organomet. Chem.*, 2000, **598**, 87–102.
- 7 J. H. Price, A. N. Williamson R.F. Schramm and B. B. Wayland, *Inorg. Chem.*, 1972, **11**, 1280–1284.
- 8 (a) C. López, X. Solans and M. Font-Bardía, *Inorg. Chem. Commun.*, 2005, **8**, 631–634; (b) C. López, A. Caubet, S. Pérez, X. Solans and M. Font-Bardía, *Chem. Commun.*, 2004, 540–541.
- 9 L. Ding, D. P. Zhou and Y. J. Wu, *Polyhedron*, 1998, **17**, 2511–2516.
- 10 S. Pérez, C. López, A. Caubet, R. Bosque, X. Solans, M. Font-Bardía, A. Roig and E. Molins, *Organometallics*, 2004, **23**, 224–236.
- 11 (a) R. Bosque, C. López, J. Sales, X. Solans and M. Font-Bardía, *J. Chem. Soc., Dalton Trans.*, 1994, 735–745; (b) C. López, R. Bosque, X. Solans and M. Font-Bardía, *New J. Chem.*, 1998, **22**, 977–982.
- 12 K. Nakamoto, *Infrared and Raman Spectra of Inorganic and Coordination Compounds*, Wiley, New York, USA, 5th edn, 1997.
- 13 G. B. Deacon and J. H. S. Green, *Spectrochim. Acta*, 1964, **24**, 845–852.
- 14 H.-U. Gremlich, *Handbook of Analytical Techniques*, 2001, 465–507.
- 15 J. Vicente, J. A. Abad, A. D. Frankland and M. C. Ramírez de Arellano, *Chem.–Eur. J.*, 1999, **5**, 3066–3075.
- 16 L. Ding, Y. J. Wu and D. P. Zhou, *Polyhedron*, 1998, **17**, 1725–1728.
- 17 (a) F. D. Rochon and M. Fakhfakh, *Inorg. Chim. Acta*, 2009, **362**, 1455–1466; (b) F. D. Rochon and M. Fakhfakh, *Inorg. Chim. Acta*, 2009, **362**, 458–470.
- 18 For reviews on ¹⁹⁵Pt-NMR: (a) B. M. Still, P. G. A. Kumar, J. R. Aldrich-Wright and W. S. Price, *Chem. Soc. Rev.*, 2007, **36**, 665–686; (b) J. R. L. Priqueler, I. S. Butler and F. D. Rochon, *Appl. Spectrosc. Rev.*, 2006, **41**, 185–226.
- 19 C. López, R. Bosque, S. Pérez, A. Roig, E. Molins, X. Solans and M. Font-Bardía, *J. Organomet. Chem.*, 2006, **691**, 475–484.
- 20 T. H. Allen, *Acta Crystallogr., Sect. B: Struct. Sci.*, 2002, **58**, 380–388.
- 21 A. I. Kitaigorodskii, *Molecular Crystals and Molecules*, Academic Press, London, UK, 1973.
- 22 E. R. Brown and J. R. Sandifer, *Physical Methods in Chemistry, Electrochemical Methods*, ed. B. W. Rossiter and H. Hamilton, Wiley, New York, USA, 1986, ch. 4, vol. 4.
- 23 R. Bosque, C. López and J. Sales, *Inorg. Chim. Acta*, 1996, **244**, 141–145.
- 24 A. D. Ryabov, G. M. Kazankov, I. M. Panyashkina, O. V. Grozovsky, O. G. Dyachenko, V. A. Polyakov and L. G. Kuzmina, *J. Chem. Soc., Dalton Trans.*, 1997, 4385–4392.
- 25 F. Stoddart, in *Comprehensive Organic Chemistry. The Synthesis and Reactions of Organic Compounds*, ed. D. Barton and W. D. Ollis, Pergamon, Oxford, UK, 1979, ch. 4, vol. 1, pp. 577–598.
- 26 P. R. R. Ranatunge-Bandarage, B. H. Robinson and J. Simpson, *Organometallics*, 1994, **13**, 500–510.
- 27 Recent contributions on this field: (a) Y. Urano, D. Asanuma, Y. Hama, Y. Koyama, T. Barrett, M. Kamiya, T. Nagano, T. Watanabe, A. Hasegawa, P. L. Choyke and H. Kobayashi, *Nat. Med.*, 2009, **15**, 104–109; (b) S. Xu, Y. Luo, R. Graeser, A. Warnecke, F. Kratz, P. Hauff, K. Licha and R. Haag, *Bioorg. Med. Chem. Lett.*, 2009, **19**, 1030–1034; (c) E. S. Lee, Z. Gao and Y. H. Bae, *J. Controlled Release*, 2008, **132**, 164–170; (d) M. Dalmou, S. Lim and S.-W. Wang, *Nano Lett.*, 2009, **9**, 160–166.
- 28 (a) M. Galanski, C. Baumgartner, K. Meelich, V. A. Arion, M. Fremuth, M. A. Jakupce, P. Schluga, C. G. Hartinger, N. Graf v. Keyserlingk and B. K. Keppler, *Inorg. Chim. Acta*, 2004, **357**, 3237–3244; (b) S. van Rijt, S. van Zutphen, H. des Dulk, J. Brouwer and J. Reedijk, *Inorg. Chim. Acta*, 2006, **359**, 4125–4129.
- 29 D. D. Perrin, W. L. F. Armarego and D. L. Perrin, *Purification of Laboratory Chemicals*, Butterworth-Heinemann, Oxford, UK, 3rd edn, 1988.
- 30 G. M. Sheldrich, *SHELXS: A computer program for determination of crystal structures*, University of Göttingen, Germany, 1997.
- 31 G. M. Sheldrich, *SHELX97: A computer program for determination of crystal structures*, University of Göttingen, Germany, 1997.
- 32 *International Tables of X-Ray Crystallography*, Kynoch Press, Birmingham, UK, vol. IV, pp. 99–100 and 149.